Iron(III) Oxide Nanoparticles as Catalysts for the Formation of Linear Glycine Peptides

Iron(III) Oxide Nanoparticles as Catalysts for the Formation of Linear Glycine Peptides

Authors

Thomas Georgelin,*[a]
Mariame Akouche,[a]
Maguy Jaber,[b]
Yuriy Sakhno,[c]
Lucrece Matheron,[d]
Frederic Fournier,[a]
Christophe Méthivier,[a]
Gianmario Martra,[c]
and Jean-Francois Lambert*[a]

[a] Sorbonne Universités, UPMC Paris 06, CNRS UMR 7197,Laboratoire de Réactivité de Surface, 4 place Jussieu, 75005 Paris, France E-mail: thomas.georgelin@upmc.fr
http://www.lrs.upmc.fr/fr/index.html
[b] Sorbonne Universités, UPMC Paris06, CNRS UMR 8220,Laboratoire d'Archéologie Moléculaire et Structurale,4 place Jussieu, 75005 Paris, France
[c] University of Torino, Nanostructured Interfaces and Surfaces –NIS Interdepartmental Centre, Department of Chemistry,via P.Giuria, 7, 10125 Torino, Italy
[d] Sorbonne Universités, UPMC Paris 06, CNRS, Institut de Biologie Paris Seine, Plateforme de spectrométrie de masse et protéomique, 7–9 quai St Bernard, 75005 Paris, France

Abstract

We have studied the behavior upon thermal activation of glycine adsorbed on three well-characterized Fe3+ oxide nanoparticle phases, maghemite, hematite, and akaganeite. The behavior of the adsorbed molecules and of the nanoparticle surfaces was monitored by four main experimental techniques, thermogravimetric analysis/differential thermal analysis (TGA/DTA), XPS, infrared spectroscopy (IR), and mass spectrometry. Glycine polymerizes by peptide bond formation in the 180–190 °C temperature range, which is somewhat higher than on previously studied oxides such as silica or alumina, giving mostly short linear peptides. At slightly higher temperatures, under an inert gas, the iron oxyhydroxides act as stoichiometric oxidants and cause oxidative degradation of the peptides formed in the previous step while they are reduced to FeO; under air, dioxygen causes reoxidation of the nanoparticle surfaces so that the overall effect is a catalytic oxidation by O2. While the direct formation of linear peptides may be beneficial to the growth of prebiotic complexity, the redox reactivity of the supports limits the temperature stability range of the oligopeptides.

Introduction

In order to understand the emergence of life on Earth, studies of the synthesis of macrobiomolecules such as proteins or oligonucleotides are essential, because they are the first bioactive molecules known. Amino acids and, more specifically, peptides and polypeptides could be the first molecules initiating the complexification of life.[1] However, their abiotic polymerization is still poorly understood. Moreover, the protein scenario[1b] in the emergence of life has to overcome kinetic and thermodynamic difficulties. In aqueous medium, peptide condensation is thermodynamically unfavored unless an activating agent is used.[2] For instance, glycine dimerization has a positive free reaction enthalpy of about 14.2 kJ/mol:[3]

$$Gly + Gly \rightarrow (Gly)2$$

It was first proposed in 1951 by Bernal that mineral surfaces could promote peptide condensations, avoiding the use of chemical activation agents such as HCN.[4] Over the years, a number of studies have been devoted to evaluate Bernal's hypothesis, and the polymerization of adsorbed or “supported“ amino acids has been observed experimentally.[5] Because of their geochemical potential, silicates, carbonates, and hydroxides were studied most often.[2a], [6] Iron oxides may also have been present on the primitive earth, but only few works have studied the interaction of amino acids and iron oxide surfaces,[5c], [7] especially in view of the many possible iron oxide and iron oxyhydroxide phases that are known to exist.

One of the first works on the interaction between amino acids and iron oxides has been published by Holm et al. who studied the adsorption of amino acids on akaganeite particles in 1983.[8] The formula of akaganeite is usually mentioned in the literature as β-FeOOH, but, in fact, it often contains a high amount of chloride ions.[9] It was synthesized in the laboratory in order to mimic particles found in deep brines of the Red Sea, which seemed to show a significant selectivity for glycine retention. Some interesting adsorption selectivity effects were observed, including the effect of acide/base speciation (zwitterions present at close to neutral pH were preferred over cations predominant under acidic conditions), but the preference for glycine in brines could not be explained.

Matrajt et al.[7a] have investigated the adsorption of amino acids on ferrihydrite (a hydrated Fe2O3, whose structure is still hypothetical[10]). Under their conditions, glycine is adsorbed on ferrihydrite with a high density (up to 1.45 molecules per nm2) but relatively low affinity. In contrast, negatively charged amino acids such as glutamate were more strongly adsorbed, which they assumed was due to favorable electrostatic interactions with the surface.

Sverjensky et al.,[11] however, proposed another adsorption model for glutamate, which is grounded in a precise geochemical analysis of previously published data concerning glutamate on an ultrahigh surface “hydrous ferric oxide“. They clearly showed that glutamate adsorption involves the formation of several

coordination complexes between the amino acid carboxylate and surface Fe3+ ions (chelating monodentate and bridging bidentate), that is inner-sphere adsorption rather than electrostatic adsorption.

Vieira et al. have studied the adsorption of cysteine onto hematite (α-Fe2O3), ferrihydrite, and magnetite (Fe3O4, a rather unstable phase containing both Fe2+ and Fe3+).[7b] The adsorption of cysteine was probably controlled by a ligand-exchange process, and significant differences were observed between the three Fe oxides. Cysteine, however, is an atypical amino acid in that it is easily transformed into cystine by a redox reaction, which complicates the analysis of its adsorption behavior on iron oxides.

Matrajt et al. were the first to evidence the condensation of amino acids to peptides on iron oxyhydroxides, more specifically on ferrihydrite. They demonstrated that glycine on ferrihydrite particles undergoes peptide condensation by heating under both wet and dry conditions without an activating agent.[7a] The formation of linear dipeptides (Gly)2 was observed after 24 h of adsorption at 95 °C. The yields were higher under dry conditions but remained very low (<0.1 %).

A more conclusive study was carried out by Shanker et al.[7c] on the interaction between glycine and alanine and iron(III) oxides. They used somewhat more severe activation conditions (up to 35 d at temperatures up to 120 °C under dry conditions) and compared the effect of one Fe3+ oxide, hematite, and two Fe3+ oxyhydroxides, goethite (α-FeOOH) and akaganeite (see above). In some cases (quite expectedly, at the highest activation temperature), almost total condensation of monomeric glycine was observed at the end of the activation period; hematite mostly gave the cyclic dimer (cyclo-Gly-Gly, also known as 2,5-diketopiperazine or DKP), while linear dimers and trimers were obtained in addition to DKP on the oxyhydroxides. Gly3 was sometimes observed in yields up to 10 %. The overall efficiency of the condensation is actually quite impressive when compared to similar syntheses attempted on other oxides,[3a] and the obtention of polymers longer than the dimers is an additional bonus.

These studies remain phenomenological: amino acid polymerization is demonstrated, but nothing is known of its mechanism or of the chemistry of the elementary steps. Moreover, the influence of adsorption processes has never been addressed.

The reactivity of glycine has of course been much studied on other mineral phases such as silica and titania nanoparticles.[12] On silica, glycine deposited from solutions can be quantitatively condensed, mostly to DKP. Many other amino acids, but not all, undergo the same reaction. This condensation is far from simple, however, and sensitively dependent on the molecular nature of the surface adsorption site and its interaction with the amino acid molecule, as recently discussed on the basis of both experimental[13] and modeling results.[14] For instance, it was known that glycine acid/base speciation plays an important role as globally neutral forms dimerize at lower temperatures than cationic or anionic forms. A more thorough examination of experimental data suggested that glycine only reacts when dehydration has proceeded to a large enough extent that zwitterions transform into the neutral form. From that point of view, a recent

study is particularly interesting: when deposition of glycine was carried out from the gas phase, an activation temperature of 130 °C was sufficient to form peptides up to 16 units long on silica or titania,[12e] and, in addition, vibrational data suggested a three-dimensional structuration of the peptides.

Following these studies, the present work focuses on the comparison of the thermal behaviors of glycine on several Fe oxyhydroxide surfaces as a function of the adsorption procedure (from the liquid or from the gas phase), in order to evidence possible mechanisms leading to glycine condensation or to its oxidation. Glycine is the simplest amino acid and was studied in detail in several works of our group.[12a], [12b], [12d] Thermogravimetry, X-ray photoelectron spectroscopy (XPS), and IR spectroscopy (in diffuse reflectance and transmission modes) have been used to understand both the interaction and the reactivity of glycine adsorbed on three different iron(III) phases, hematite (α-Fe2O3), maghemite (γ-Fe2O3), and akaganeite (β-FeOOH).

Results

(1) Iron Oxide and Oxyhydroxide Nanoparticles: Synthesis and Characterization

The size and morphology of the maghemite γ-Fe2O3 nanoparticles (Mgh) were observed by transmission electron microscopy (TEM). Mgh appears as spherical nanoparticles with a mean diameter of 5.5±1.2 nm (Figure 1, Figure S1 in the Supporting Information). As expected, the distribution is well fitted with a log-normal law.[15] Hematite (Ht) appears as ill-defined nanoparticles with a mean diameter of 120±10 nm and akaganeite (Aka) as rod-like nanoparticles with average dimensions of 500 nm × 80 nm. Thus, the aspect ratio for Aka nanoparticles is around 0.16.

Figure 1.

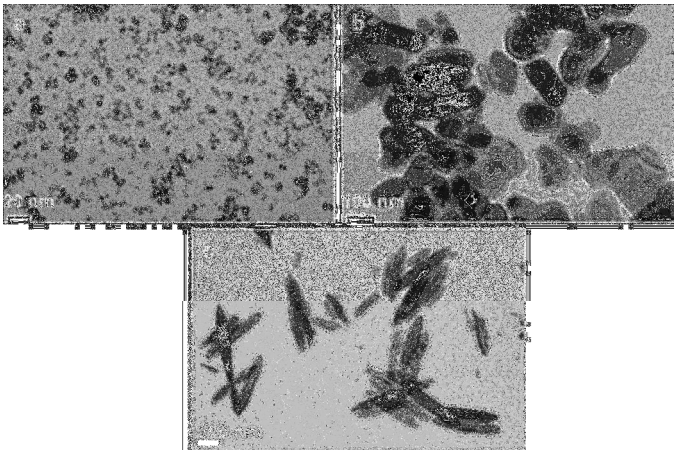

TEM images of maghemite nanoparticles extracted from ferrofluid solution (Mgh, a), scale bar 20 nm; hematite nanoparticles, (Ht, b), scale bar 100 nm; and akaganeite nanoparticles, (Aka, c), scale bar 200 nm.

The X-ray diffraction patterns (Figure 2) at room temperature confirm the synthesis of pure phases of maghemite, hematite, and akaganeite. The indexation was performed according to JCPDS files. Maghemite and hematite are poorly crystalline, whereas akaganeite is highly crystalline.

Figure 2.

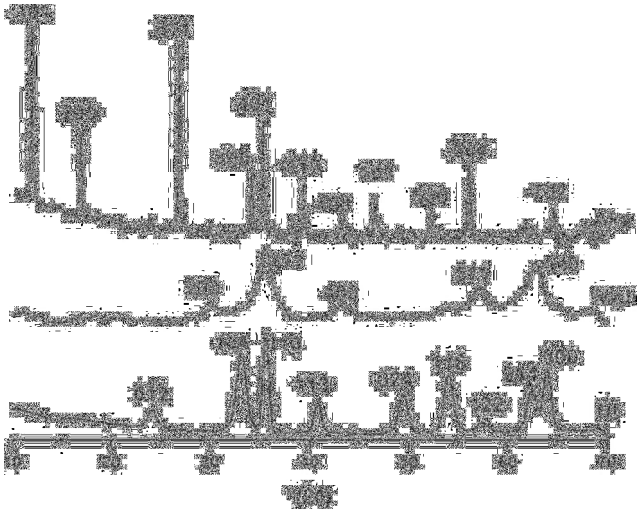

XRD pattern of Ht, Mgh, and Aka samples. Assignment according to JCPDS data numbers: JCPDS 04-0755, JCPDS 33-0664, and JCPDS 34-1266, respectively.

Specific surface areas are 145 m2/g, 45 m2/g, 165 m2/g for Mgh, Ht, and Aka, respectively. While the value measured for Mgh is compatible with a calculation based on the particle size, the value for Ht appears several times higher than the calculation and that for Aka about 10 times higher. This seems to indicate that the latter two materials have a significant fraction of their surface area in micro- and mesopores.

According to the adsorption and desorption isotherms, they show intraparticle porosity with a small portion of mesoporosity judging from the presence of a hysteresis (see Supporting Information).

After adsorption of glycine by the wet impregnation process, no new diffraction peaks were apparent on XRD patterns, and in particular there was no crystalline glycine, as opposed to the observations made, for example, on the Gly/SiO2 system.[12a] The first interpretation that comes to mind is that all the glycine molecules from aqueous solution are adsorbed on the surface of the oxide minerals. However, on the basis of the measured surface areas, the surface densities resulting from the deposition of 10 % of glycine on the support would be 5.5 glycine/nm2, 18.0 glycine/nm2, and 4.9 glycine/nm2 on Mgh, Ht, and Aka, respectively. Given that a physical monolayer is estimated at 2 glycine/nm2 at the most, it follows that glycine is probably adsorbed in amorphous multilayers on the surface of the iron oxides.

(2) Glycine on Iron Oxides: Thermogravimetry

Gly/Mgh

In order to characterize the thermal reactivity of adsorbed glycine, thermogravimetric analyses were carried out. Glycine-free maghemite nanoparticles were first analyzed as a reference. Figure 3 presents the differential thermogravimetry (DTG) analysis of Mgh under air flow. A strong endothermic peak around 70 °C can be assigned to the loss of physisorbed water from the surface (about 2.7 % by weight or 6.5 water molecules per nm2).

Figure 3.

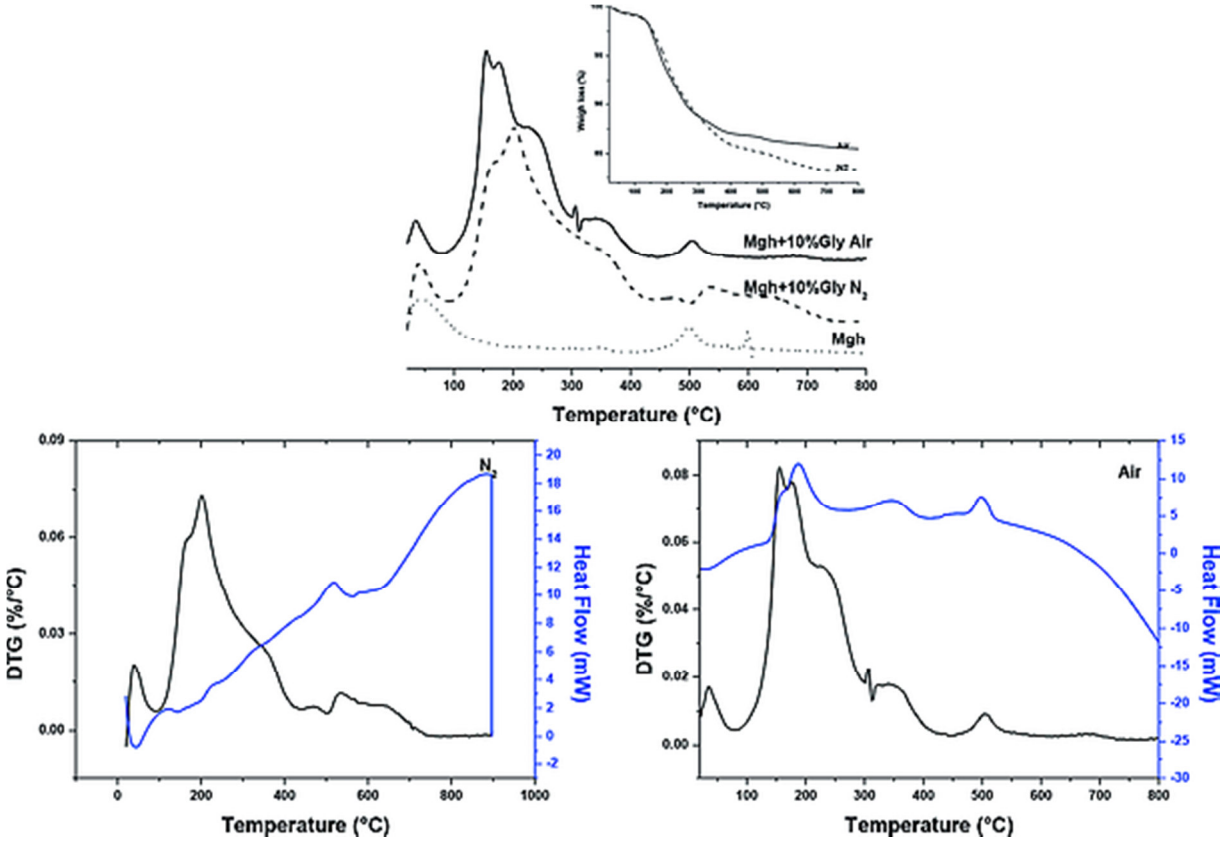

Top: DTG of Mgh under air flow, Gly/Mgh under air flow, and Gly/Mgh under nitrogen flow (TG curves in inset). Bottom: comparison of DTG (black) and DTA (blue) profiles of Gly/Mgh under air and under nitrogen flow.

A strongly exothermic event is clearly identified on the differential thermal analysis (DTA) curve at 500 °C. It corresponds to the maghemite–hematite phase transition.[16] This reorganization is accompanied by strong sintering of the particles, and a significant part of the surface hydroxy groups of maghemite are condensed to oxide ions in the newly formed lattice. This condensation causes water elimination, corresponding to 1.5 % of the initial weight, or alternatively to the elimination of 7 Fe–OH groups per nm2 of initial surface, a reasonable figure.

For Gly/Mgh, under air, several peaks are observed in the 100–400 °C region (which did not show any significant events for the raw Mgh support), with maxima at 155, 176, 223, and 345 °C. After correction for the blank, the total weight loss corresponding to these peaks is 10.9 %, a value in good agreement with the amount of glycine introduced. At higher temperatures, the DTG and DTA curves are superimposable to

those of raw Mgh, and in particular the phase transition at 500 °C is still observed. We may conclude that all of the deposited glycine has been eliminated at about 440 °C, while the support was still maghemite.

When the TG is carried out under N2, although the overall DTG profile is rather similar, the final weight loss is higher by 1.8 %; furthermore, the maghemite/hematite transition is not observed anymore, indicating that the support has been significantly modified. We have reason to believe that the global reaction leading to glycine elimination is oxidative. Under air, dioxygen acts as the oxidant, but in its absence this role is played by the Fe3+ ions in the Mgh support, and Fe2O3 is reduced to FeO, with the loss of 1/2 oxide for each reduced Fe ion (XPS analysis confirms this interpretation as discussed below). If indeed the additional weight loss of 1.8 % can be attributed to this phenomenon, it is easy to calculate that the elimination of glycine involves an oxidation of, on average, 1.5 electrons per glycine molecule; alternatively, 18.0 % of the Fe3+ ions are reduced to Fe2+.

This concerns the global reaction that is completed at 440 °C. It is also interesting to focus on the first steps, observed at low temperature. One may wonder if glycine molecules start with undergoing a condensation to peptides, similar to what is observed on other supports.[5d] The DTA data do show an initial endotherm (as expected for a condensation) superimposed on higher-temperature exothermic reactions. In order to shed more light on this observation, we have analyzed by mass spectrometry (MS) the gases evolved during TG under N2. A signal at 18 amu (H_2O^+) was observed with a main peak at 160 °C, while at higher temperatures the main signals were at 44 amu (CO_2^+) and 46 amu (NO_2^+). These observations comfort the idea of an initial condensation event resulting in the evolution of water, immediately followed by deep oxidation events. A word of caution is in order here, however. We also observed, at higher temperatures, a signal at 43 amu that could correspond to etheneamine ($CH_2{=}CH{-}NH_2^+$), which would involve a reductive reaction of glycine. Therefore, it is likely that the high-temperature reactions of glycine are rather complex. A complete understanding of these redox reactions would necessitate an in-depth study of Gly/Mgh samples with variable glycine loadings, which is beyond the scope of the present contribution.

We did, however, synthesize a sample with higher glycine loading in order to confirm the hypothesis of glycine oxidation involving oxygen from the mineral support. For 30 % Gly/Mgh, we observed again a smaller residual mass when the sample was heated under N2 flow up to 800 °C as compared to the same sample treated under air flow. In this case, the difference amounted to 9.6 % of the Fe_2O_3 mass, which is indeed higher than that for 10 % Gly, although not proportionately.

Gly/Ht

The TGA of bulk hematite [(Figure 4), curve labeled as Ht] shows only two significant peaks at 182 (athermic) and 216 °C. The latter one is clearly endothermic and represents a weight loss of around 0.8 %. We have no immediate explanation for this; it could be due to the elimination of some surface impurity from the synthesis medium. Dehydration of the surface Fe–OH groups of hematite has been reported to start at 210 °C,[17] but this event is normally not so sharp as the one observed here. In the case of Gly/Ht, several peaks can be correlated with the presence of glycine in the sample. Under air, the main events are

at 187, 257, and 343 °C and correspond to a weight loss of 9.9 %, very close to the introduced amount of glycine. Under N2, the profile is more complex; significant weight losses can be observed up to 715 °C, and the integrated weight loss is 3.2 % higher than under air. Once again, the oxidative degradation of glycine is accompanied by reduction of the support (about 32.0 % of the initial Fe3+; or 3 electrons per glycine molecule).

Figure 4.

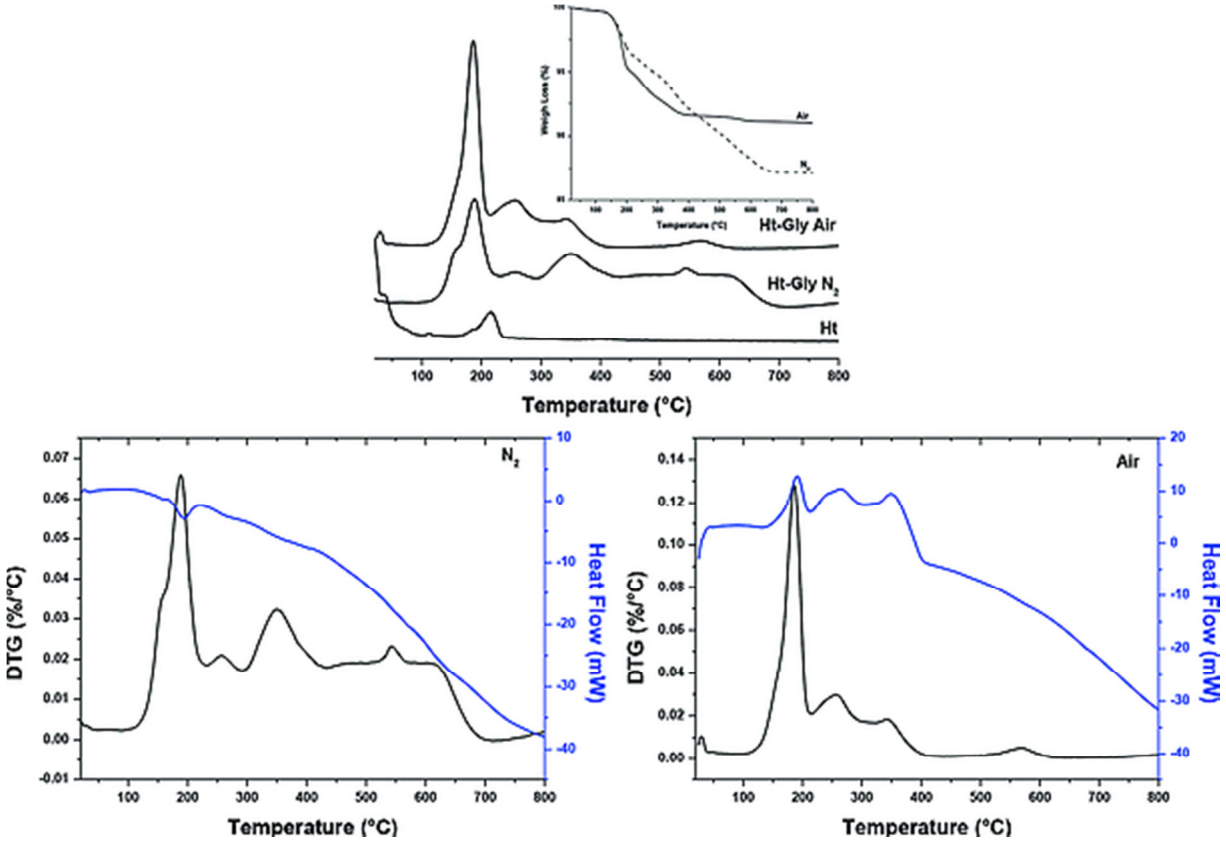

Top: DTG of Ht under air flow, Gly/Ht under air flow, and Gly/Ht under nitrogen flow (TG curves in inset). Bottom: comparison of DTG (black) and DTA (blue) profiles of Gly/Ht under air and under nitrogen flow.

It is of note that the first peak, at 188 °C, with a shoulder at 155 °C, corresponds to a definitely endothermic step. These maxima fall in the temperature range previously reported for amino acid condensation on other supports. Furthermore, they are well separated enough from events at higher temperature to allow their approximate quantification. The weight loss corresponding to this interval is around 2.7 % of the support mass, close to the theoretical value (2.4 %) expected for the total condensation of glycine according to: Gly + Gly → cyclo-Gly–Gly + 2 H2O (the same value would be obtained for the condensation to infinite linear polyglycine).

In summary, the evidence for initial peptidic condensation, at temperatures lower than subsequent degradation reactions, is stronger than for that on maghemite.

Gly/Aka

Akaganeite is different from the previous two supports in that it undergoes significant transformations in the low-temperature range that is of interest to us (Figure 5). Indeed, akaganeite is not an oxide but an Fe3+ oxyhydroxide with the formula FeOOH. The constitutional hydroxides are unstable at medium temperatures and condense to give oxides according to:

2 FeOOH → α-Fe2O3 (hematite) + H2Ogas,

Figure 5.

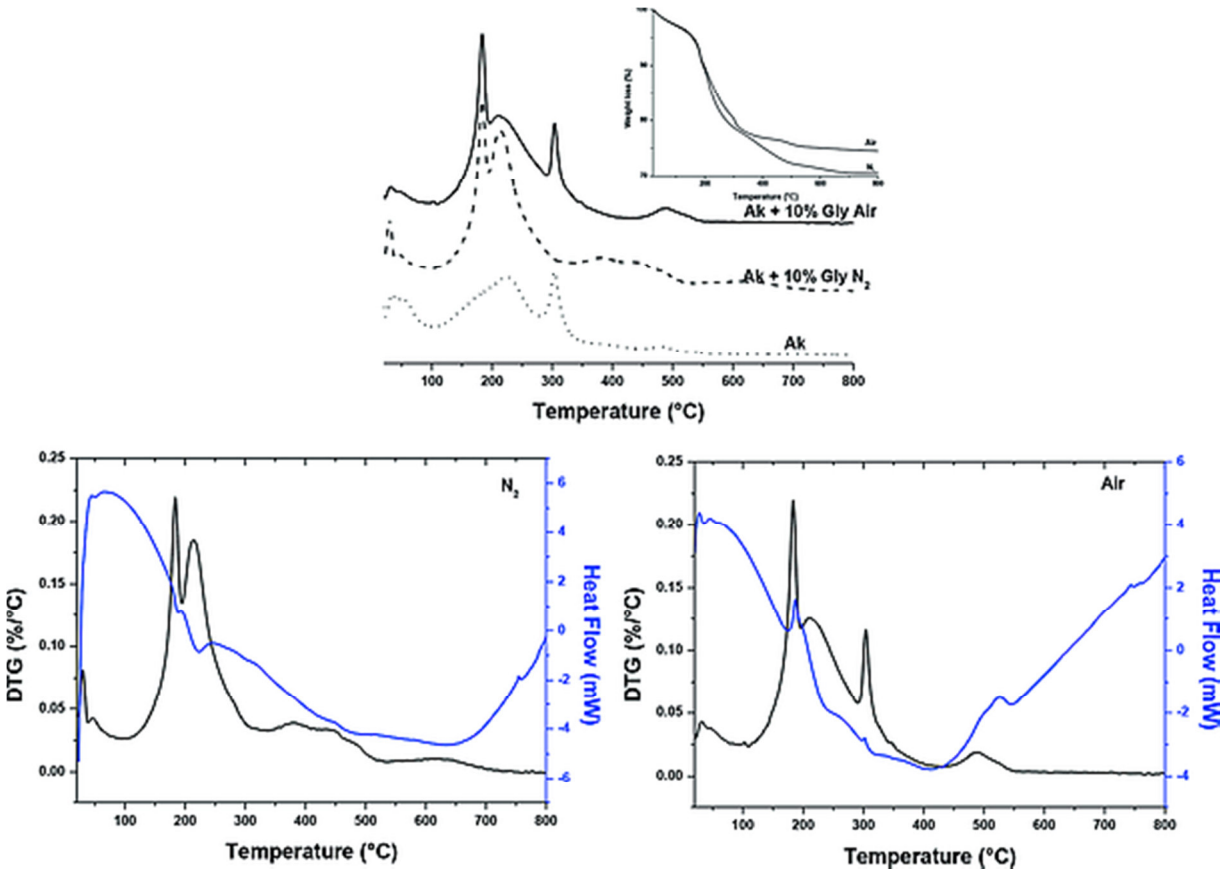

Top: DTG of Aka under air flow, Gly/Aka under air flow, and Gly/Aka under nitrogen flow (TG curves in inset). Bottom: comparison of DTG (black) and DTA (blue) profiles of Gly/Aka under air and under nitrogen flow.

a reaction, which should result in a weight loss of 10.1 % (with respect to the initial weight). In a rather old study, Babcan et al.[18] indeed observed a total weight loss of about 10 % in two clearly separate steps at 225 and 302 °C, the first being endothermic and the second exothermic. Our sample showed the same two events (maxima at 224 and 304 °C, both endothermic, however), but with a weight loss of 15.5 %; the weight loss corresponding to the first event alone was closer to 10 %. This shows that the thermal evolution of akaganeite is more complicated than expected and should be investigated in its own right (probably, the substitutional chloride ions can participate in thermal reactions); this is not, however, the main purpose of the present contribution.

For Gly/Aka under air, the most conspicuous feature was a sharp exothermal event peaking at 183 °C, not present for the raw support. Following that, both support dehydroxylation and glycine degradation occurred simultaneously. Starting from 535 °C (i.e., at the phase transition), the mass evolution of Gly/Aka was superimposable to that of bare akaganeite. We may surmise that at this temperature both samples have transformed into Fe2O3. The weight loss of Gly/Aka from 100 to 535 °C, corrected for the weight loss of the raw support in the same range, should then give the amount of adsorbed glycine. In fact, this estimate gives 7.4 %, which is of the same order but significantly inferior to the introduced amount (10.0 %).

Coming back to the sharp peak at 183 °C, one wonders if it can be assigned to glycine condensation as was done for a peak at the same temperature in Gly/Mgh. In the case of Gly/Aka, however, the peak is now exothermic, and, in addition, the corresponding weight loss (about 3.3 %) is significantly too high with respect to the theoretical value for condensation (2.4 %).

For Gly/Aka under N2, we noticed that the glycine-correlated peak at 183 °C is still present, but endothermic; the support-correlated peak at 304 °C is totally absent; and the total integrated weight loss is 5.5 % higher than that under air, indicating reduction of the support (about 69.0 % of the initial Fe3+).

Thermogravimetric results are more ambiguous with akaganeite than with the other two supports, but overall they are also compatible with glycine condensation overlapping with redox transformations involving the support.

(3) Glycine Adsorbed from the Liquid Phase: XPS

The N (1s) signals of supported glycine samples and their thermally activated products can be decomposed into two components at 399.9–400.3 eV and 401.8–401.9 eV, respectively. In many studies of functionalized surfaces, two peaks in these respective ranges are attributed to the unprotonated and protonated forms of the amine moiety, respectively, –NH2 and –NH3+. In particular, for glycine adsorbed on various surfaces, the –NH2 function corresponds to the nonionic molecule and –NH3+ to the zwitterion.[19]

Initially, glycine speciation is tilted toward the neutral form on all iron oxide surfaces under our analysis conditions (Figure 6). On maghemite nanoparticles the NH3+/NH2 ratio is around 0.4.

Figure 6.

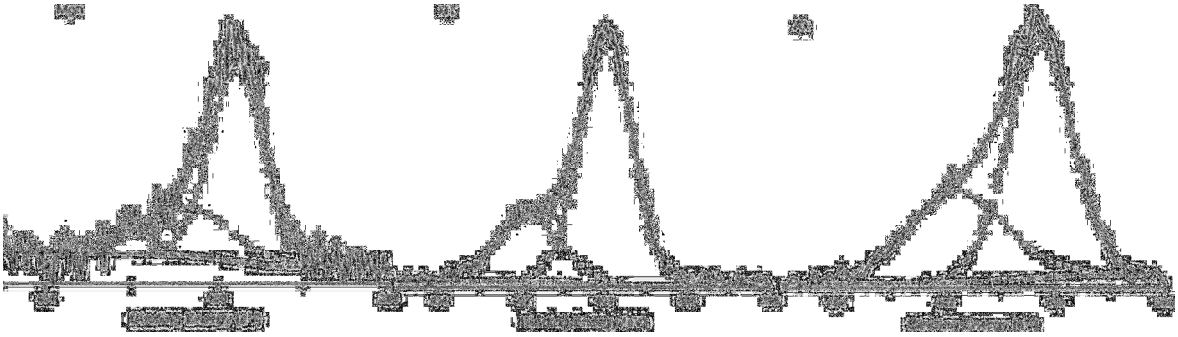

XPS spectra at the N (1s) edge of Gly/Mgh, Gly/Ht, and Gly/Aka, showing the signal decomposition into two components. NH3+ contribution (401.8 eV); amide/NH2 contribution (400.3 eV).

On hematite and akaganeite, these ratios are 0.28 and 0.65, respectively. We have observed a similar phenomenon for other supported amino acids;[20] while in the aqueous solution used for deposition, glycine was certainly zwitterionic, the stabilization of the zwitterionic form usually crucially depends on the number of water molecules interacting with the amino acid,[21] and outgassing in the XPS chamber removes enough water to stabilize the nonionic form instead.

We have paid attention to the evolution of the N (1s) signal during the thermal activation of Gly/Mgh (Table 1).

Table 1. Relative contribution of (NH_2 + amide) to the N (1s) spectrum of Gly/Mgh activated at different temperatures

	r.t.	**150 °C**	**200 °C**	**250 °C**
NH_2	70 %	100 %	68 %	47 %

Initially, the proportion of NH2, and thus of nonionic glycine in the sample is 70 %. Heating under vacuum may cause a shift in the nonionic glycine/zwitterion speciation, but also amide condensation and other degradation reactions as mentioned above. The N (1s) signal of the amide nitrogen in bulk peptides has been reported to be between 400.4 (dipeptides) and 400.6 eV (polypeptides);[22] for the linear dipeptide Gly–Gly deposited on Si, the terminal amine, presumably protonated to NH3+, gave a signal at 402.2 eV and the amide of the same molecule at 400.6 eV.[23] Introducing a third component in the decomposition of our spectra did not result in an improvement of the fit; we can only distinguish between a first signal corresponding to terminal –NH3+ and a second one corresponding to (NH2 + amide). The proportion of the latter increases to 100 % at 150 °C, that is in the temperature range of peptide condensation. At higher temperature, during the oxidation process, it starts decreasing; at 250 °C, the main signal observed is in the –NH3+ range. It probably corresponds to some intermediate products in the oxidative degradation of peptides: at the same time, during thermal activation, the N/Fe atomic ratio decreases form 2.5 to 0.8 %, indicating the desorption of a large part of the final degradation products.

Figure 7 shows the signal of the Gly/Mgh series in the Fe (2p) region. The binding energies for peaks 2p1/2 and 2p3/2 are observed at 724.7 and 711.2 eV, respectively. These values, and particularly the difference in binding energy ΔE between the two maxima (13.5 eV) are compatible with pure maghemite, rather than partly reduced surface phases such as Fe_3O_4, according to Banerjee et al.[24] This is confirmed by the existence of a shake-up satellite peak at 719.5 eV (ΔE with 2p3/2 = 8.3 eV).[25] Thus, the nanoparticles used for this study initially consisted in pure maghemite, and this was not altered by glycine deposition.

Figure 7.

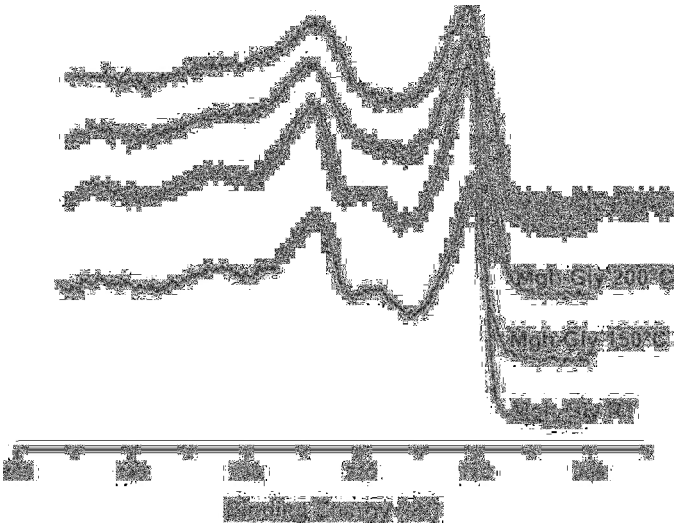

XPS spectrum at the Fe (2p) edge of Gly/Mgh activated under vacuum at different temperatures.

Analyses of the Fe 2p3/2 spectrum during thermal activation show the growth of a contribution below 710 eV, corresponding to a ferrous (Fe^{2+}) iron species.[25] At the same time, the satellite peak due to Fe^{3+} decreases to the point of disappearing at 250 °C (Figure 7). It seems that the majority of the surface Fe^{3+} ions are converted into Fe^{2+}. This reduction of the support surface is also apparent from the O (1s) spectrum. The O (1s) signal contains three components: acidic oxygen at 532.3 eV, hydroxy/carboxylate at 531.5 eV, and oxide oxygen at 529.9 eV. The ratio of the latter component to the area of Fe (2p) peaks has been used in order to estimate the O/Fe ratio. For untreated samples, the XPS O/Fe ratio is around 1.5, a value in good agreement with the Fe_2O_3 stoichiometry of maghemite. After glycine adsorption, this ratio does not change (remember that the oxygen atoms of the glycine molecule are observed separately from the oxide oxygen atoms). During heat treatment under vacuum, the O/Fe atomic ratio decreases from 1.5 to 1.1, indicating the reduction of the surface from an Fe_2O_3 stoichiometry to one that is close to FeO (Figure 8). Thus, the partial reduction by reaction with glycine that was deduced from TG results is confirmed by XPS; indeed iron seems to be completely reduced in the surface region.

Figure 8.

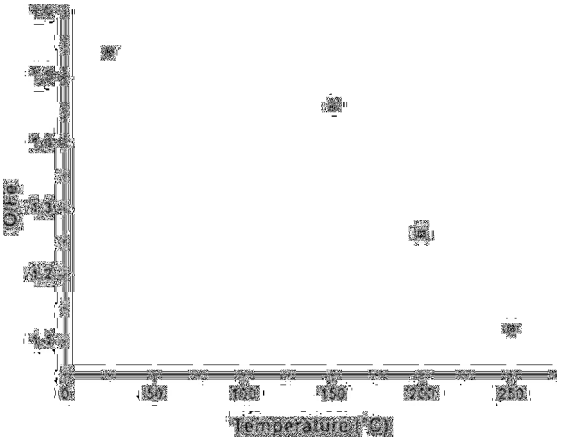

Evolution of the O/Fe atomic ratio during thermal activation of Gly/Mgh.

(4) Glycine on Iron Oxyhydroxydes: IR Spectroscopy

Adsorption of Glycine from the Liquid Phase

The spectra of Gly/Mgh, Gly/Ht, and Gly/Aka are shown in Figures S3, S4, S5, respectively, in the Supporting Information. Table 2 proposes assignments for the main adsorption bands observed in the 1000–1800 cm–1 range (in which the iron oxide supports are mostly transparent), on the basis of known band positions in bulk α-glycine.[6i]

Table 2. DRIFT spectroscopy (main vibrational bands of bulk glycine and adsorbed glycine samples); n.o. = not observed

Assignement	**Bulk glycine (KBr pellet)**	**Gly/Mgh**	**Gly/Ht**	**Gly/Aka**
$\delta_{as'}NH_3^+$	1611	n.o.	n.o.	n.o.
$\nu_{as}COO^-$	1596	n.o.	1590	n.o.
$\nu_{as}CO_2 + \delta_sNH_3$	1525, 1505	n.o.	1522	n.o.
δ_sCH_2	1445	1440	1443	1444
ν_sCO_2	1413	1380	1412	1413
$\omega CH_2 + \varrho_{op}NH_3$	1334	1320	1332	1332
$\nu CN + \omega CH_2 + \varrho_{ip}NH_3$	1133	1133	1133	1133
$\tau CH_2 + \varrho_{op}NH_3$	1113	1114	1113	1113
$\nu C–N$	1034	1036	1034	1035

Several bands in the supported Gly systems have positions very similar to bulk glycine. This indicates that the glycine molecules are in a weak interaction with the surface, such as hydrogen bonding (in bulk glycine, too, the individual molecules are involved in a network of H bonds with their neighbors[6i]), but not establishing strong bonds such as coordination to surface ions. An exception is observed for the carboxylate group vibration in Gly/Mgh, which shifts significantly, from 1412 (in bulk glycine) to 1380 cm–1. This shift could be interpreted as the consequence of a strong interaction between the maghemite surface and glycine, possibly through the formation of coordinative bonds between the carboxylate moiety and surface

Fe3+ ions. It is observed neither for Gly/SiO2[12a] nor for the other two Fe oxyhydroxide supports (Table 2).

We next tried to determine how the vibrational spectra of supported glycine samples evolve with thermal activation. We present our data as difference spectra, that is the spectrum at the indicated temperature has been corrected by subtracting the spectrum at 30 °C.

For Gly/Mgh (Figure 9), in situ thermal activation first causes an increase of a signal centered at 1697 cm–1, which is most manifest at 150 °C. This might be due to the appearance of an amide I vibrational band, as there are some indications of glycine condensation (endothermic peak at 150 °C in DTG). However, if that was the case, a positive signal corresponding to an amide II band should have appeared at the same time at around 1580 cm–1, and such a signal is not observed. Starting at 120 °C, negative signals are visible as well in the difference spectra and become more and more prominent up to 250 °C. Their positions correspond to the most intense bands of glycine, which means that we are mostly witnessing the progressive elimination of glycine. Indeed this temperature region corresponds to the most intense DTG peaks in the thermogram of Gly/Mgh. Water loss may also contribute to the negative peak in the 1630 cm–1 region. However, this negative peak does not appear before 120 °C. Therefore, the most likely explanation is that water elimination is already largely completed at 30 °C under vacuum.

Figure 9.

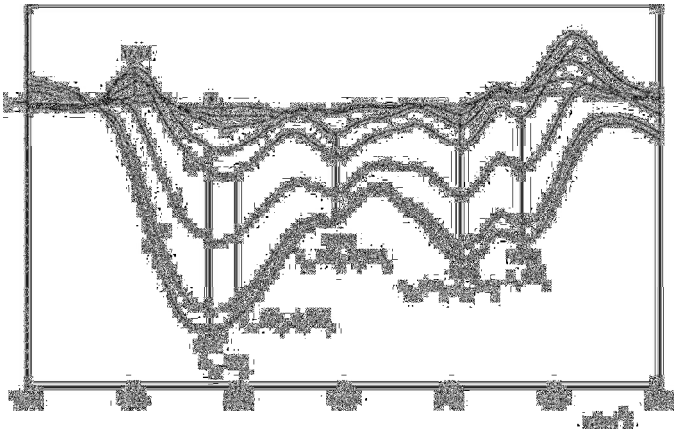

Difference DRIFT spectra of Gly/Mgh (corrected for spectrum at 30 °C) under in situ thermal activation at (a) 50 °C, (b) 70 °C, (c) 100 °C, (d) 150 °C, (e) 190 °C, (f) 200 °C, (g) 220 °C, (h) 250 °C.

At higher temperatures, the carbonyl band decreases significantly, whereas the component at 1717 cm–1 decreases to a lesser extent. On hematite, the thermal behavior is different (Figure 10).

Figure 10.

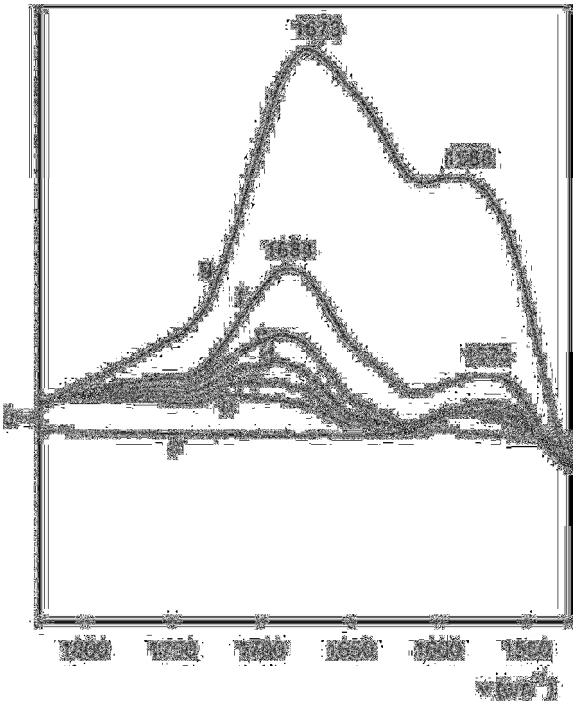

Left: difference DRIFT spectra of Gly/Ht (corrected for spectrum at 30 °C) under in situ thermal activation at (a) 50 °C, (b) 70 °C, (c) 100 °C, (d) 150 °C, (e) 200 °C, (f) 220 °C, (g) 250 °C. Right: decomposition of the amide I band of Gly/Ht 150 °C.

Up to 220 °C, which corresponds to the completion of the first and most intense DTG peak, two components increase simultaneously, with maxima at around 1680 and 1580 cm–1. They could correspond to the amide I and amide II bands, confirming the formation of peptides in the thermal event that peaks at 187 °C in the DTG. Between 150 and 220 °C, the amide I band consists of two components at 1680 and 1630 cm–1. Possible reasons for the existence of these two components will be considered in the discussion. At the highest temperatures, the band maximum shifts to 1673 cm–1, which corresponds to the amide link of the cyclic dimer DKP.[6h] The presence of DKP is also suggested by a band at 1469–1478 cm–1 in the subtracted spectra (not shown), which could be the breathing mode of the DKP cycle.[6h]

A component at around 1715 cm–1 is necessary for a correct fit of the high-energy side of the amide I band. None of the canonical peptide structures gives an amide I band at such a high wavenumber, and thus it could be due to degradation products. Indeed, for Gly/SiO2, Lambert et al.[12a] have observed a band at 1716 cm–1 after activation at relatively high temperatures; in this study, it was probably a product of DKP thermal evolution and was not investigated further.

After heating to 250 °C, the proportion of the component at 1680 cm–1 increases significantly compared to the band at 1705 cm–1, which would mean that most of the glycine molecules that had not yet transformed at 150 °C condense to form peptides (including DKP) rather than other degradation products. On akaganeite, thermal activation induces the progressive increase of amide I and II bands (Figure 11).

Figure 11.

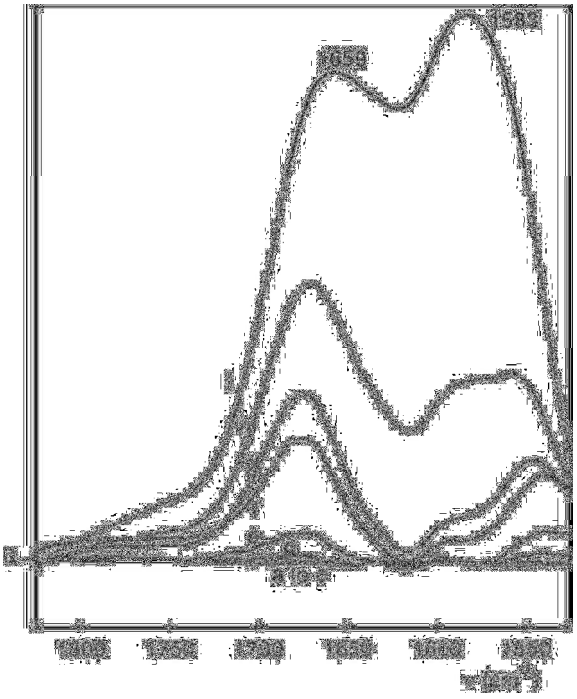

Left: difference DRIFT spectra of Gly/Aka (corrected for spectrum at 30 °C) under in situ thermal activation at (a) 50 °C, (b) 70 °C, (c) 100 °C, (d) 150 °C, (e) 170 °C, (f) 190 °C, (g) 200 °C, (h) 220 °C, (i) 250 °C. Right: decomposition of the amide I band of Gly/Aka at 150 °C. Bottom: decomposition of the amide I and II bands of Gly/Aka at 250 °C.

At 150 °C, the amide I band is centered at 1659 cm–1 and can be fitted with three components at 1635, 1675, and 1691 cm–1 (the introduction of a fourth band does not improve the quality of the fit). No band is observed at around 1710 cm–1 up to 250 °C, indicating the stability of glycine-derived peptides on akaganeite. The presence of DKP is suggested by a band at 1460 cm–1, in the same way as that on maghemite. At 250 °C (Figure 11), the components of the amide I vibrational band are centered at 1641, 1677, and 1700 cm–1. A contribution at 1749 cm–1 probably corresponds to the νCO vibration of COOH groups in products of degradation as on maghemite, but it remains a minor component. The shift of the vibrational band could be due to an amide band in another environment as observed in the case of hematite, or alternatively to the decrease of the proportion of DKP (1670 cm–1). Nevertheless, the position of the amide I band shifts from 1660 cm–1 at 150 °C to 1600 cm–1 at 200 °C. After thermal activation at 200 °C, the intensity in the 1750–1500 cm–1 region decreases as a consequence of water and probably glycine desorption. It should be added that in this particular case intensity changes are also observed in the 3000–3600 cm–1 region, corresponding to OH stretching modes (not shown). They correspond to the thermal modifications of structural OH in akaganeite. In particular, a significant overall decrease is observed starting from 220 °C, when the condensation of OH groups that accompanies the transition to hematite is already underway (see TG results).

Adsorption of Glycine from the Vapor Phase

The adsorption of Gly was also carried out from the vapor phase on dehydrated samples. This method seemed particularly interesting for the formation of long peptide oligomers in view of the results obtained

on SiO2 and TiO2, where polymers up to (Gly)16 were obtained.[12e] The IR spectra in the 1775–1200 cm–1 range of Gly adsorbed in this way on Mgh, Ht, and Aka, keeping the coverage below the monolayer (see Exp. Sect.), are shown in Figure 12, panels A–C.

Figure 12.

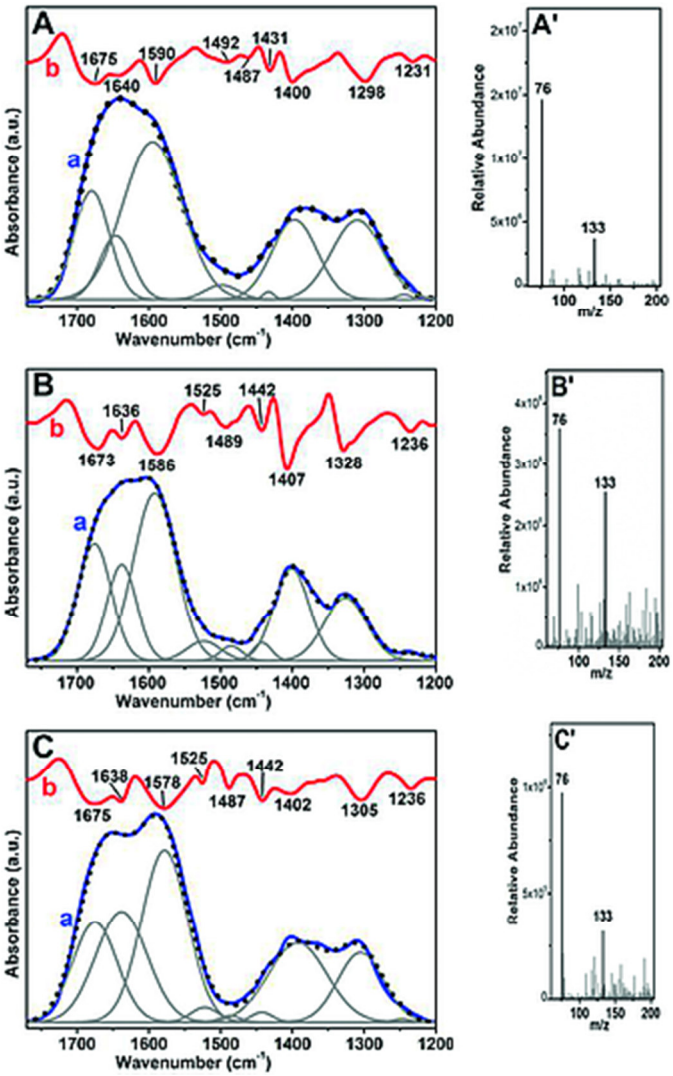

IR spectra [(a) curves, blue], in the 1775–1200 cm–1 range, of Gly adsorbed from the vapour phase on Mgh (panel A), Ht (panel B), and Aka (panel C). The spectra of the bare specimens before Gly adsorption were subtracted as a background. In each panel, above the spectrum is its second derivative [(b) curve, red], whilst below are the sub-bands resulting from its decomposition (grey curves). The sum of the sub-bands is the dotted line overimposed to the experimental spectrum. Panels A'–C': HR mass spectra of the solutions resulting from washing (with milliQ water) of the corresponding sample used for the IR measurement.

The spectral profiles exhibit two groups of bands in the ranges of 1750–1500 and 1450–1200 cm–1, both of them resulting from the superposition of several components. A decomposition of the profiles was carried out, where the number and position of fitted sub-bands were chosen in correspondence with the minima of the second derivative of the experimental spectra (Figure 12, top curve in each panel; this method could not be applied for Figures 9, 10, and 11 in view of the less favorable signal/noise ratio). Most of the

components obtained in this way can be assigned to Gly monomers in zwitterionic form (Table 3), with slight differences in position and relative intensity among the three cases that can likely be assigned to weak interactions (such as H-bonding) with different types of surface sites.

Table 3. Assignment of IR sub-bands [frequency (cm^{-1})] resulting from the decomposition of the spectra of Gly adsorbed from the vapour phase on Mgh, Ht and Aka. ν_{asym}: antisymmetric stretching; ν_{sym}: symmetric vibration; δ: bending; γ: out-of-plane deformation

Frequency	**Material**	**Assignment**
1675	Mgh	amide I
1673	Ht	
1675	Aka	
1640	Mgh	$\delta_{asym}NH_3^+$
1636	Ht	
1638	Aka	
1590	Mgh	$\nu_{asym}COO^-$
1586	Ht	and
1578	Aka	amide II
1492	Mgh	νC–N + δC–N–H
1525	Ht	and
1525	Aka	$\delta_{asym}NH_2$
1487	Mgh	$\delta_{sym}NH^{3+}$
1489	Ht	
1487	Aka	
1431	Mgh	δCH_2
1442	Ht	
1442	Aka	
1400	Mgh	$\nu_{sym}COO^-$
1407	Ht	
1402	Aka	
1298	Mgh	δC–N–H + νC–N
1328	Ht	
1305	Aka	
1231	Mgh	γCH_2
1236	Ht	
1236	Aka	

Since Gly molecules in the gas phase are in the nonionic form, this indicates that when Gly molecules are adsorbed on the surface of the three materials, they are isomerized from nonionic to zwitterionic as observed and modeled for Gly on hydroxyapatite nanoparticles.[26] The component at the highest frequency (ca. 1675 cm–1) cannot be assigned to monomers, however, and it falls in a range where the vCO signal of amide bond species (amide I band) is expected.

In this case, the amide II mode might contribute to the low-frequency side of the sub-band at about 1580 cm–1. Confirmation of the formation of peptides was provided by mass spectrometry analysis of the solutions resulting from the washing with ultrapure water of the samples used for the IR measurements (see below).

(5) Glycine on Iron Oxides: Mass Spectrometry

The nature of the organic molecules present on the surfaces of the iron oxide nanoparticles was studied by mass spectrometry before and after thermal activation (200 °C) under N2 flow.

After glycine adsorption from the liquid phase on maghemite followed by drying, a peak of protonated monomeric glycine GlyH+ was detected at m/z = 76.04 amu, together with a peak at m/z = 151.071 amu and, surprisingly, one of a minor amount (<5 %) of protonated glycylglycine Gly–GlyH+ at m/z = 133.060 amu. No trace of cyclic glycine was observed. Note that the peak at 151.07 amu could correspond to an adduct between protonated and unprotonated glycine, (GlyH+,Gly), or alternatively an adduct between Gly–GlyH+ and one water molecule; we favor the first hypothesis since this peak seems to be correlated with the intensity of the GlyH+ signal, rather than with that of the dimer. After activation at 200 °C under N2, a similar spectrum was recorded, the only difference being a slight increase (by a factor of 2) in the relative intensity of Gly–GlyH+ related to GlyH+.

After adsorption from the liquid phase on hematite, the same three signals are observed as those on maghemite. After activation, the proportion of GlyH+ decreases, while linear Gly–GlyH+ increases and linear Gly3H+ appears. Higher polymers are not detectable, but DKP (cyclo-Gly–Gly) is present.

On akaganeite, after drying, we again observed GlyH+, (GlyH+,Gly), and the linear dimer Gly–GlyH+, the latter in higher amounts than that on the other two supports (80 % of the GlyH+ signal). After activation, the proportion of the linear dimer increases, but no trace of DKP is present.

Mass spectrometry was also used to identify the organic species present on the samples prepared by the gas-phase adsorption method. After adsorption, mass spectrometry revealed the presence of GlyH+ and Gly–GlyH+ on all three materials (Figure 12). Thermal activation at 200 °C promoted the Gly condensation reaction resulting in the formation of longer oligomers in Gly/Ht [GlyH+, Gly–GlyH+, (Gly3)H+, and (Gly4)H+] and Gly/Aka [Gly/Ht; GlyH+, (Gly)2H+, and (Gly)3H+], while the amino acids and peptides appear to be destroyed in Gly/Mgh (neither oligomers nor monomers in mass spectra).

Discussion

We have observed the same general trends in reactivity for glycine adsorbed from the aqueous solution and from the gas phase on the three ferric oxyhydroxides maghemite, hematite, and akaganeite. Namely,

we believe that on all three phases the amino acid molecules can condense to form peptide bonds at rather low temperatures; but they can also, at only slightly higher temperatures, take part in redox reactions involving ions from the support that result in complete (or almost complete) oxidative degradation.

As expected from previously published results,[7a] TGA, DRIFT, and XPS analyses strongly suggest that on all three iron oxyhydroxide surfaces the formation of peptides from Gly adsorbed from aqueous solution can happen from around 180 to 190 °C. TGA indeed indicates the elimination of water at around 180 °C, and by DRIFT spectroscopy, amide band formation is clearly observed at these temperatures. For hematite and akaganeite, this confirms the results of Shanker;[7c] for maghemite, which had not been previously investigated, the spectroscopic evidence for peptide bond formation is less compelling.

According to TGA, the temperature of glycine condensation is slightly higher than that on a silica surface, where condensation occurs at 160 °C under the same analytical conditions.[12b], [12d] One possible explanation could be that the adsorption mechanism is different. On silica, glycine interacts with the surface only through hydrogen bonding, while on iron oxyhydroxides coordination bonding may be suspected.[26] It is well known that there often exists an optimum strength of the molecule–surface interaction for efficient catalysis (Sabatier's principle; this lies at the origin of “volcano plots“ for catalytic activity as a function of reagent–catalyst bonding strength). We have previously proposed that, for the catalysis of amide bond condensation, the optimum interaction was through H-bonding. However, the evidence for coordinative bonding of glycine is lacking. Spectroscopic evidence exists only on maghemite; but since the adsorption from the liquid phase is multilayered, a minority of glycine molecules could strongly interact with the surface, and their signal could be undetected because of the existence of a large amount of more weakly bound molecules.

After peptide condensation, the second set of reactions occurring after 220 °C, when the temperature is raised, results in complete degradation of the supported organic molecules (glycine and/or peptides derived from it) and is completed before 500 °C in most cases. On other supports such as silica, total degradation of the supported organic molecules is also observed in an intermediate temperature range (typically from 200 to 600 °C), due to a series of pyrolysis reactions that are imperfectly understood.[6e], [27] On Fe oxyhydroxides, however, the reactions involved are clearly different in that they comprise redox reactions between glycine and the support. This is most clearly evidenced by the reduction of Fe^{3+} to Fe^{2+} accompanied by oxide loss when working under N_2 flow, which is almost complete in the surface region as witnessed by XPS. It follows that glycine and/or peptides must be oxidized in the same event, both stoichiometrically and electronically. Several different oxidation reactions must be occurring in parallel and to different extents in different samples as shown by our quantification of TGA results.

This type of redox reactions between organic molecules and reducible transition-metal oxides is well known from the literature on heterogeneous catalysis, especially as a step of the Mars-van-Krevelen catalytic mechanism (see below). It is generally interpreted as involving (surface) sites that can exist in two forms, oxidized (*O) and reduced (*), and would be written as follows, with R being the reduced form of the organic molecule and RO its oxidized form:

*O + Rgas → * + ROgas

Adaptation to other stoichiometry is trivial:

x *O + Rgas → x* + ROx,gas

We can be more specific: for the systems under study, *O represents a lattice oxide ion, or Fe3+–O2––Fe3+, and the corresponding reduced site * represents Fe2+–VO–Fe2+, where VO is an oxide vacancy. Thus, the oxidation of previously synthesized peptides (Rads), which starts at 200 °C, may be written as [Equation (1)]:

display math(1)

Under N2 flow, this stoichiometric (as opposed to catalytic) reaction is the only one that occurs, and a considerable amount of oxide ions are lost to the oxidized degradation products ROx that are eliminated in the gas phase.

On the other hand, when dioxygen is present in the gas phase, such as under air flow, it may react with the reduced form of the catalytic sites to regenerate their oxidized form as [Equation (2)]:

display math(2)

The two steps, (1) and (2), then constitute a closed kinetic sequence whose sum is simply the catalytic oxidation of Rads to ROx,gas, while the catalytic sites cycle between their oxidized and reduced forms.

The difference in weight loss between TG under air and under N2 represents the amount of reducible catalytic sites that take part in step (1). It is considerably higher than the amount of surface-exposed oxides as quantification shows that between 20 and 50 % of the initial Fe3+ oxyhydroxides are reduced to FeO, depending on the sample. This means that the point defects formed at the surface in step (1) – oxide vacancies and Fe2+ substitutional ions – are able to migrate into the bulk.

Reduction of Fe oxyhydroxides by several organic molecules at moderate temperatures has been reported before. Thus, a study by Rosmaninho et al.[28] focused on the capacity of ethanol to reduce iron oxide surfaces. Ethanol reduced hematite to magnetite starting at 350 °C and magnetite to FeO starting at 500 °C. In contrast, in our work, glycine reduced hematite, probably directly to FeO, at temperatures as low as 200

°C. Other molecules are even more efficient than glycine: Fe_2O_3 nanoparticles could act both as a stoichiometric oxidant (in the absence of O_2) and as an oxidation catalyst (in the presence of O_2) for carbon monoxide (CO) in a manner reminiscent of their action on glycine;[29] catalytic oxidation could be observed even at room temperature for highly dispersed Fe_2O_3.[30]

The temperature from which the weight loss under N_2 becomes more important than under air flow may be taken as a rough estimate of the propensity of the support to oxidize glycine or its peptides. For maghemite this point is observed at 300 °C and for hematite at 450 °C. This order is in good agreement with DRIFT results, as Gly/Mgh spectra only indicate the inception of the appearance of the amide I band, which was soon overshadowed by the degradation of glycine; in contrast, the spectra of Gly/Ht indicate that peptides were fully formed before oxidative degradation started to any noticeable extent. This seems also to be the case on akaganeite (Gly/Aka), but the surface chemistry of the latter support at low temperatures is more complicated than for the other two phases we studied.

When Gly adsorbs from the vapor phase, it interacts with the dehydrated surface in nonionic state only, while in the liquid phase speciation favors the zwitterion Gly±. However, its state is determined more by the extant surface hydration conditions than by the initial speciation. IR spectroscopy shows that vapor-phase-deposited Gly is zwitterionic after deposition on an incompletely outgassed surface. Conversely, for liquid-phase-deposited Gly, XPS measurements, which necessitate equilibration in a high-vacuum chamber, indicate a coexistence of glycine in nonionic and zwitterionic states in a 70:30 ratio; this ratio even incresaes to 100:0 upon thermal activation at 100 °C. Thus, irrespective of its state in the deposition medium, adsorbed glycine is a zwitterion when the surface is hydrated (i.e., up to at least 150 °C) and nonionic when it is dehydrated (around 200 °C when heated in gas flow, but already at 100 °C when heated in ultrahigh vacuum).

On other supports such as silica, the formation of peptide bonds between adsorbed amino acids only starts when the surface is sufficiently dehydrated so that speciation shifts from the zwitterion to the nonionic form. Our results show that the same is true on hematite and akaganeite: a significant amount of peptide bonds are formed between 150 and 200 °C, as evidenced by a specific thermal event in TG, the appearance of amide bonds in IR spectra, and the MS analyses of desorption solutions. This is in agreement with previous results;[7c] in contrast, on maghemite, which had not been studied before, the possible formation of peptides is obscured by the inception of their oxidative degradation. This negative result does not mean that maghemite surfaces are inefficient towards peptide condensation, but rather that they are too active for oxidation reactions (catalytic, or stoichiometric depending on the atmosphere). At any rate, maghemite would not provide a viable pathway for the formation of prebiotic peptides, because their window of stability would be too restricted.

It must be underlined that the possibility of peptidic condensation is determined by the hydration state of the surface (water activity), and that similar degrees of dehydration may be achieved at lower temperatures if the treatment is carried out for longer times. Thus, our results do not contradict those of Shanker et al. who observed glycine (and alanine) polymerization at temperatures in the range of 50 to 120

°C, but with much slower kinetics than ours (e.g. 1 % transformation at 50 °C on akaganeite after 35 d). This may also explain why some amount of the Gly–Gly dimer was already observed in our samples after the drying step (70 °C overnight).

Regarding the nature of the peptides formed, they are essentially linear and rather short, with akaganeite apparently favoring slightly longer polymers; these essential trends were independently observed for the two sets of samples prepared by deposition from the liquid phase or from the vapor phase. In particular, the cyclic dimer DKP remained a minority component, in strong contrast with what happens on silica where it is the only observable polymerization product for samples prepared by the liquid-phase adsorption method.[5c], [12a] Contrarily, very long polymers (up to 15 Gly moieties) were observed for samples prepared by vapor-phase adsorption. Shanker et al.[7c] also generally observed condensation products consisting of short linear polymers, up to the trimer, although in some of their experimental conditions the cyclic dimer became more prominent; Matrajt et al. observed Gly–Gly and (Gly)3 upon heating of Gly/ferrihydrite at 95 °C for a few days. It seems therefore that, while the ability to promote peptidic condensation is shared with many mineral surfaces, the outcome of this reaction strongly depends on the nature of the surface; on silica, but not on iron oxyhydroxides, it also depends on the deposition procedure.

Linear peptides are “interesting”, because cyclic DKP is sometimes considered as a dead end in the formation of longer, biologically significant peptides. Another interesting feature is suggested by the specific shape of the amide I and II bands observed for the samples from liquid deposition. Several components at distinct wavelengths are needed to model the band shapes correctly in Gly/Ht and Gly/Aka. In long peptides and proteins, this might be indicative of classical three-dimensional structure such as α-helices and β-sheets, and even for the oligomers formed in Gly/SiO_2 and Gly/TiO_2, β-sheet structuring has been claimed on the basis of amide band shapes.[12e] In our samples (Gly/Ht and Gly/Aka), the short sizes of the oligomers do not, of course, allow the formation of such extensive structures. However, specific patterns of H-bonding, which are the ultimate reason for the amide band shifts in tertiary protein structures, are possible even for short oligomers (and even for monomers for that matter). Thus, specific intermolecular interactions could explain the evolution of the amide I vibrational band during thermal activation:[31] small linear peptides could be self-assembled on the surface, by H bonds with their neighbors, but also with surface OH groups and/or co-adsorbed water molecules. Of course, any evidence of peptide structuring is very important, because it could constitute a step towards the generation of functional biomolecules, and, from a more fundamental point of view, because it suggests a kind of molecular recognition taking place at the interfaces. This three-dimensional structuring is probably facilitated by the presence of water in our sample prepared from the liquid phase. In contrast, the adsorption of Gly from the vapor phase in the absence of water does not result in any particular morphology of the amide I band, indicating the absence of specific intermolecular interactions.

Conclusions

The thermal reactivity of glycine on Fe^{3+} oxyhydroxides is clarified by the present work. First, it is confirmed that these materials, like other mineral phases, promote peptide bond formation between

supported amino acids upon mild thermal activation, although somewhat higher temperatures are needed than, for example, on silica.

Second, the temperature range allowing stability of the peptides formed in this manner is limited as the supports can take part in redox reactions where the supported organic molecules are oxidized, while the surface region of the nanoparticles is reduced to a stoichiometry close to FeO. Under an inert gas, the solid supports act as stoichiometric redox reagents at temperatures as low as 200 °C; when dioxygen is present in the gas phase, it reoxidizes the surface so that the Fe oxyhydroxide particles globally act as an oxidation catalyst (Mars-van-Krevelen mechanism). Maghemite is the most reactive support for glycine oxidation, and therefore the least useful for peptide formation.

Third, the products of glycine condensation consist of short linear peptides (Gly2 to Gly3). This is in contrast with supports such as silica where DKP is the predominant product. Linear oligoglycines are predominant irrespective of whether glycine was deposited from the liquid or from the vapor phase.

Finally, at least in the case of liquid-phase deposition on hematite and akaganeite, the amide bands seem to consist of several components. The explanation proposed on related systems, based on tertiary structuring of peptide chains (β-sheets, α-helices), cannot be transposed here because of the small lengths of the peptide chains. However this might indicate a definite H-bonding pattern between short peptides formed by self-assembly at moderate temperatures, and any hint of structuring is an important element in evaluating the potential of mineral surfaces to help to produce complex biochemical systems; we intend to carry out a more precise study of H-bonded structures on mineral interfaces in the future.

Experimental Section

Materials: Glycine (99 %), $FeCl_3$, $FeCl_2$, and ammonia solution (27 %) were purchased from Sigma–Aldrich. In solution, glycine (Gly) can exist as three different species (H_2Gly^+, $HGly^\pm$, and Gly^-), connected by acid/base speciation with pKa values of 2.4 and 9.7. In the bulk, $HGly^\pm$ is predominant.

Nanoparticles Synthesis: Maghemite (γ-Fe_2O_3) nanoparticles were obtained by heating magnetite powder at 350 °C in an oven under air flow for 12 h. The point of zero charge (PZC) of maghemite nanoparticles was around 7.5.[32] The abbreviation Mgh is used for maghemite nanoparticles. Parent magnetite (γ-Fe_3O_4) nanoparticles were prepared by co-precipitation of Fe^{2+} and Fe^{3+} ions under alkaline conditions according to the well-known procedure described by Massart et al.[15] Briefly, to a solution of $FeCl_3$ (35 mL, 0.1 mol/L) in water was added a solution of $FeCl_2$ (1.7 mL, 1 mol/L) in water, and the solution was then acidified to a pH about 2 with HCl. Precipitation of magnetite nanoparticles was induced by addition of ammonia solution (3 mL, 10 mol/L). The resulting black suspension was stirred at room temperature for 10 min, and the precipitate was magnetically separated. The flocculate of particles was washed five times with distilled water. Hematite nanoparticles (α-Fe_2O_3) were prepared by heating maghemite nanoparticles at 500 °C for 24 h. The PZC of hematite nanoparticles was around 10.0.[33] The abbreviation Ht is used for

hematite nanoparticles. Akaganeite nanoparticles (β-FeOOH) were prepared by a hydrolysis process. $FeCl_3$ (4.0 g, 25 mmol) was dissolved in distilled water (250 mL). The pH was adjusted to 1.3 with HCl, and the mixture was aged in a polypropylene vial at 70 °C for 48 h. The yellow powder that precipitated was then washed several times with water and dried at 70 °C overnight. The PZC of akaganeite nanoparticles was around 7.5.[6g] The abbreviation Aka is used for akaganeite nanoparticles.

Adsorption Procedure from the Liquid Phase: In a typical adsorption experiment, to iron oxyhydroxide (100 mg) was added an aqueous solution of glycine (100 µL) at a suitable concentration to obtain the desired loading (generally, 10 % by weight related to the mass of support). After equilibration at room temperature for 30 min, the mixture was dried under air flow in an oven at 70 °C overnight. This procedure, which does not involve a step of separation between the aqueous solution and the solid support and consequently results in deposition of all the initially introduced glycine molecules, is called incipient wetness impregnation as in the literature on heterogeneous catalysis. The three samples obtained in this way are called Gly/Mgh, Gly/Ht, and Gly/Aka.

Adsorption Procedure from the Vapor Phase: Details on the operative procedure with related schemes are reported in the Supporting Information of a report of Martra et al.[12e] In summary, self-supporting pellets of the Fe oxyhydroxide of interest and of Gly were placed in a conventional IR cell for measurements in the transmission mode. The pellet of Gly was placed in a sample holder in one of two adjacent parts of the cell devoted to thermal treatments, while the pellet of oxyhydroxide was kept free to be moved from these parts to the bottom of the cell equipped with CaF_2 windows, for IR spectroscopic measurements. At first, the oxyhydroxide pellet was placed in the first part of the cell devoted to thermal treatments, and outgassed at 140 °C for 1 h to remove surface species such as H_2O, carbonates, etc. absorbed due to previous contact with air. The outgassing temperature represented the best compromise among attainment of a high surface dehydration level (target: 95 %), need to avoid the conversion of materials from oxyhydroxides to oxides, and temperature reached during the subsequent Gly sublimation step. After outgassing, the oxyhydroxide pellet was moved in the IR-transparent part of the cell, and its spectrum was recorded. Then, the sample was moved close to the Gly pellet in a third part of the cell that was then heated at 140 °C for 10 min. Gly vapors were produced close to the oxyhydroxide pellet. During this process, the cell was kept open toward a liquid-nitrogen trap, in order to remove water resulting from possible Gly condensation reactions. The sample in contact with Gly vapor was then cooled to room temperature and moved back to the cell part devoted to IR measurements. The (contact with Gly vapor/IR spectra recording) sequence was repeated until bands resulting from the adsorption of Gly attained an intensity similar to signals exhibited by a reference sample impregnated with an aqueous Gly solution, prepared in order to have ca. 1 Gly molecule per nm^2.

X-ray Powder Diffraction (XRD): X-ray powder diffraction (XRD) was carried out on the final solids with a Bruker D8 Advance diffractometer by using Cu-Kα radiation (λ = 1.5404 Å). XRD patterns were recorded between 10 and 70° with a step size of 0.05°, and the time per step was 3 s.

Thermogravimetric Analysis (TG-DTA): TGA of the samples was carried with a TA Instruments Waters LLC, with an SDT Q600 analyzer, by using a heating rate β of 5 °C/min under dry air or dry nitrogen flow (100 mL/min). Values of weight losses were usually normalized to the final weight at 800 °C, unless otherwise mentioned.

X-ray Photoemission Spectroscopy Analyses (XPS): The samples were analyzed at different temperatures by X-ray photoemission spectroscopy with a SPECS GmbH (Berlin, Germany) Phoibos 100–5MCD hemispherical analyzer and a monochromatized Al-Kα X-ray source (1486.6 eV). After recording a broad-range spectrum (pass energy 50 eV), high-resolution spectra were recorded for the N (1s), C (1s), O (1s), and Fe (2p) core levels (pass energy 10 eV). High-resolution XPS conditions were fixed: "Fixed Analyser Transmission" analysis mode, 7 × 20 mm entrance slit leading to a resolution of 0.1 eV for the spectrometer, and an electron-beam power of 400 W (15 kV and 27 mA). The spectra were fitted with the Casa XPS v.2.3.15 software (Casa Software Ltd., UK) and by applying a Gaussian/Lorentzian (G/L) ratio of 70:30.

Infrared Spectroscopy. (a) Diffuse Reflectance Mode (DRIFT): Spectra were recorded with a Bruker IFS 66 V spectrometer (2 cm–1 resolution, 256 scans/spectrum, MCT detector). A powdered sample (ca. 40 mg) was placed inside a heated crucible located in a Thermo Spectra-Tech high-temperature cell equipped with two ZnSe windows and under Ar flow. The reference spectrum was recorded with KBr (Fluka, purity >99.5 %). (b) Transmission Mode: Infrared spectra of the samples were recorded with a Bruker IFS 28 (2 cm–1 resolution, 256 scans/spectrum, DTGS detector) in the transmission mode. The lab-made cell used, equipped with CaF2 windows (see above) was permanently attached to a conventional vacuum line (residual pressure 1 × 10–4 mbar), allowing thermal treatments and desorption/adsorption experiments to be carried out in situ. The optical thickness of the oxyhydroxyde pellets was in the range of 4–6 mg/cm2.

Transmission Electron Microscopy (TEM): TEM images were obtained with a JEOL 100CX2 microscope operating at 65 keV. Evaluation of the size and aspect ratio of nanoparticles was carried out by using the ImageJ software.

Mass Spectrometry (MS): For mass spectrometry analyses, MilliQ H2O (100 µL) was added to the samples (powders or crushed pellets used for samples contacted with Gly vapors), which were gently vortexed for 5 min, then centrifuged at ca. 7600 g for 5 min. The supernatant was recovered, and formic acid (FA) was added to a final concentration of 1 vol.-%. The supernatant was analyzed as is or diluted up to 30 times in order to reach a satisfactory signal. The samples were analyzed with an LTQ Orbitrap XL (Thermo Fisher Scientific) mass spectrometer equipped with an NSI source in direct infusion with a 100 µL Hamilton syringe at a flow rate of 1 µL/min. Before each sample, the baseline signal (1 % FA) was monitored until it was stable and the signal from the previous sample was sufficiently removed. All data were recorded in the Orbitrap analyzer, with a scan range from 50 to 500 amu at a resolution of 60000. The AGC target was set to 2 × 105, the maximum injection time to 100 ms. The signal was monitored until stability, and then recorded for 1 min. Measured m/z values were averaged over the whole acquired spectra.

Supporting Information (see footnote on the first page of this article): Figures S1–S9.

Acknowledgements

M. A. was supported by a Ph.D. grant from the Ile-de-France region, under the DIM-ACAV program.

[1] a) A. Brack, Pure Appl. Chem. 1993, 65, 1143–1151; b) K. Plankensteiner, H. Reiner, B. M. Rode, Curr. Org. Chem. 2005, 9, 1107–1114.
[2] a) T. Georgelin, M. Jaber, H. Bazzi, J.-F. Lambert, Orig. Life Evol. Biosph.2013, 43, 429–443; b) T. Georgelin, M. Jaber, T. Onfroy, A.-A. Hargrove, F.
Costa-Torro, J.-F. Lambert, J. Phys. Chem. C 2013, 117, 12579–12590.
[3] a) J.-F. Lambert, Orig. Life Evol. Biosph. 2008, 38, 211–242; b) E. L. Shock,Geochim. Cosmochim. Acta 1992, 56, 3481–3491.
[4] J. Bernal, The physical basis of life, Routledge and Kegan Paul, London, 1951.
[5] a) D. A. M. Zaia, Amino Acids 2004, 27, 113–118; b) N. Lahav, Heterog. Chem. Rev. 1994, 1, 159–179; c) J. F. Lambert, Geochim. Cosmochim. Acta 2010, 74, A557–A557; d) J.-F. Lambert, M. Jaber, T. G eorgelin, L. Stievano, Phys. Chem. Chem. Phys. 2013, 15, 13371–13380; e) V. A. Basiuk, T. Y. Gromovoy, E. G. Khil'chevskaya, Orig. Life Evol. Biosph. 1995, 25, 375–393.
[6] a) H. J. Cleaves II, A. M. Scott, F. C. Hill, J. Leszczynski, N. Sahai, R. Hazen, Chem. Soc. Rev. 2012, 41, 5502–5525; b) M. Jaber, J.-F. Lambert, J. Phys. Chem. Lett. 2010, 1, 85–88; c) M. Bouchoucha, M. Jaber, T. Onfroy, J.-F. Lambert, B. Xue, J. Phys. Chem. C 2011, 115, 21813–21825; d) M. Jaber, T. G eorgelin, H. Bazzi, F. Costa-Torro, J.-F. Lambert, G. Bolbach, G. Clodic,
J. Phys. Chem. C 2014, 118, 25447–25455; e) O. Poch, M. Jaber, F. Stalport, S. Nowak, T. Georgelin, J.-F. Lambert, C. Szopa, P. Coll, Astrobiology 2015, 15, 221–237; f) T. Georgelin, S. Bombard, J.-M. Siaugue, V. Cabuil, Angew. Chem. Int. Ed. 2010, 49, 8897–8901; Angew. Chem. 2010, 122, 9081; g) T. Georgelin, V. Maurice, B. Malezieux, J.-M. Siaugue, V. Cabuil, J. Nanopart.
Res. 2010, 12, 675–680; h) S. Balme, R. Guegan, J.-M. Janot, M. Jaber, M. Lepoitevin, P. Dejardin, X. Bourrat, M. Motelica-Heino, Soft Matter 2013, 9, 3188–3196; i) M. Lepoitevin, M. Jaber, R. Guegan, J.-M. Janot, P. D ejar-din, F. Henn, S. Balme, Appl. Clay Sci. 2014, 95, 396–402.
[7] a) G. Matrajt, D. Blanot, Amino Acids 2004, 26, 153–158; b) A. Vieira, G. Berndt, I. de S ouza Junior, E. Di Mauro, A. Paesano, H. de Santana, A. da Costa, C. Zaia, D. Zaia, Amino Acids 2011, 40, 205–214; c) U. Shanker, B. Bhushan, G. Bhattacharjee, Kamaluddin, Orig. Life Evol. Biosph. 2012, Eur. J. Inorg. Chem. 2017, 198–211 www.eurjic.org © 2017 Wiley-VCH Verlag GmbH & Co. KGaA, Weinheim211 42, 31–45; d) K. Naka, Y. Tampo, Y. Chujo, J. Organomet. Chem. 2007, 692, 436–441; e) P. Pandey, C. K. Pant, K. Gururani, P. Arora, S. Kumar, Y. Sharma, H. D. Pathak, M. S. Mehata, Orig. Life Evol. Biosph. 2013, 43, 331–339.
[8] N. G. Holm, M. J. Dowler, T. Wadsten, G. Arrhenius, Geochim. Cosmochim. Acta 1983, 47, 1465–1470.
[9] G. Naren, H. Ohashi, Y. Okaue, T. Yokoyama, J. Colloid Interface Sci. 2013, 399, 87–91.
[10] F. M. Michel, L. Ehm, S. M. Antao, P. L. Lee, P. J. Chupas, G. Liu, D. R.
Strongin, M. A. A. Schoonen, B. L. Phillips, J. B. Parise, Science 2007, 316, 1726–1729.
[11] D. Sverjensky, C. M. Jonsson, C. L. Jonsson, H. J. Cleaves, R. Hazen, Environ. Sci. Technol. 2008, 42, 6034–6039.
[12] a) M. Meng, L. Stievano, J. F. Lambert, Langmuir 2004, 20, 914–923; b)M. Meng, L. Stievano, J. F. Lambert, Chin. J. Catal. 2005, 26, 393–398; c)
A. Rimola, S. Tosoni, M. Sodupe, P. Ugliengo, ChemPhysChem 2006, 7, 157–163; d) L. Stievano, L. Y. Piao, I. Lopes, M. Meng, D. Costa, J.-F. Lambert, Eur. J. Mineral. 2007, 19, 321–331; e) G. Martra, C. Deiana, Y. Sakhno,I. Barberis, M. Fabbiani, M. Pazzi, M. Vincenti, Angew. Chem. Int. Ed. 2014, 53, 4671–4674; Angew. Chem. 2014, 126, 4759.
[13] J.-F. Lambert, L. Stievano, I. Lopes, M. Gharsallah, L. Piao, Planet. Space Sci. 2009, 57, 460–467.
[14] A. Rimola, D. Costa, M. Sodupe, J.-F. Lambert, P. Ugliengo, Chem. Rev. 2013, 113, 4216–4313.
[15] R. Massart, IEEE Trans. Magn. 1981, 17, 1247–1248. [16] Y. H. Chen, J. Alloys Compd. 2013, 553 , 194–198.

[17] J. Jayashainy, P. Sagayaraj, J. Alloys Compd. 2015, 626, 323–329.
[18] J. Babčan, J. Krištin, J. Therm. Anal. 1971, 3, 307–310.
[19] a) J. Kim, P. Seidler, L. S. Wan, C. Fill, J. Colloid Interface Sci. 2009, 329;b) G. Tzvetkov, G. Koller, F. P. Netzer, Surf. Sci. 2012, 606, 1879–1885; c) A. Shavorskiy, T. Eralp, K. Schulte, H. Bluhm, G. Held, Surf. Sci. 2013, 207, 10–19.
[20] M. Jaber, M. Bouchoucha, L. Delmotte, C. Méthivier, J.-F. Lambert, J. Phys. Chem. C 2011, 115, 19216–19225.
[21] a) F. R. Tortonda, J. L. Pascual-Ahuir, E. Silla, I. Tunón, Chem. Phys. Lett. 1996, 260, 21–26; b) C. M. Aikens, M. S. Gordon, J. Am. Chem. Soc. 2006, 128, 12835–12850; c) S. X. Tian, X. Sun, R. Cao, J. Yang, J. Phys. Chem. A 2009, 113, 480–483.
[22] D. T. Clark, J. Peeling, L. Colling, Biochim. Biophys. Acta, Protein Struct. 1976, 453, 533–545.
[23] L. Zhang, A. Chatterjee, K. T. Leung, J. Phys. Chem. C 2011, 115, 14155–14163.
[24] a) I. Banerjee, Y. B. Khollam, C. Balasubramanian, R. Pasricha, P. P. Bakare, K. R. Patil, A. K. Das, S. V. Bhoraskar, Scripta Mater. 2006, 54, 1235–1240; b) J. Lu, S. Yang, K. M. Ng, C.-H. Su, C.-S. Yeh, Y.-N. Wu, D.-B. Shieh, Nanotechnology 2007, 18.
[25] A. P. Grosvenor, B. A. Kobe, M. C. Biesinger, N. S. McIntyre, Surf. Interface Anal. 2004, 36, 1564–1574.
[26] A. Rimola, Y. Sakhno, L. Bertinetti, M. Lelli, G. Martra, P. Ugliengo, J. Phys. Chem. Lett. 2011, 2, 1390–1394.
[27] T. Georgelin, M. Jaber, F. Fournier, G. Laurent, F. Costa-Torro, M.-C. Maurel, J.-F. Lambert, Carbohydr. Res. 2015, 402, 241–244.
[28] M. G. Rosmaninho, F. C. C. Moura, L. R. Souza, R. K. Nogueira, G. M. Gomes, J. S. Nascimento, M. C. Pereira, J. D. Fabr is, J. D. Ardisson, M. S. Nazzarro, K. Sapag, M. H. Araújo, R. M. Lago, Appl. Catal., B 2012, 115–116, 45–52.
[29] P. Li, D. E. Miser, S. Rabiei, R. T. Yadav, M. R. Hajaligol, Appl. Catal., B 2003, 43, 151–162.
[30] H. Y. Lin, Y. W. Chen, W. J. Wang, J. Nanopart. Res. 2005, 7, 249–263.
[31] H. Torii, T. Tatsumi, T. Kanazawa, M. Tasumi, J. Phys. Chem. B 1998, 102, 309–314.
[32] J.-C. Bacri, R. Perzynski, D. Salin, V. Cabuil, R. Massart, J. Magn. Magn. Mater. 1990, 85, 27–32.
[33] Y. T. He, J. Wan, T. Tokunaga, J. Nanopart. Res. 2008, 10, 321–33